Christian Frey[1]
Institute of Propulsion Technology,
German Aerospace Center (DLR),
Linder Höhe, 51147 Cologne, Germany
e-mail: christian.frey@dlr.de

Graham Ashcroft
Institute of Propulsion Technology,
German Aerospace Center (DLR),
Linder Höhe, 51147 Cologne, Germany
e-mail: graham.ashcroft@dlr.de

Michael Müller
Institute of Propulsion Technology,
German Aerospace Center (DLR),
Linder Höhe, 51147 Cologne, Germany
e-mail: mi.mueller@dlr.de

Jens Wellner
Institute of Propulsion Technology,
German Aerospace Center (DLR),
Linder Höhe, 51147 Cologne, Germany
e-mail: jens.wellner@dlr.de

Analysis of Turbomachinery Averaging Techniques

In this paper, various averaging techniques commonly used in turbomachinery applications are analyzed. It is shown how the work average relates to Miller's mechanical work potential and that it is, in a certain way, consistent with Hartsel's cooled turbine efficiency. It is found that a key to understand these approaches is to analyze the impact that entropy variations at inflows have on them. Second-order asymptotics of mixing entropy are used to establish a close relationship between flux and work averages. It is found that the mixing entropy asymptotic due to entropy modes is identical for both averages. The work average, along with Miller's mechanical work potential analysis, is as optimistic as the entropy average for vorticity and acoustic modes, but as pessimistic as the flux averaging for entropy variations. This explains why mechanical work potential-based analysis is pessimistic about the inflow and thus optimistic about the efficiency of a turbine for high entropy variations in the inflow, e.g., in the presence of hot streaks or film cooling. Radial averaging techniques are discussed and their impact on turbine performance is shown. Our findings are illustrated by means of the analysis of steady and unsteady flow simulations of a 1.5 stage turbine configuration. [DOI: 10.1115/1.4056057]

Keywords: computational fluid dynamics (CFD), fluid dynamics and heat transfer phenomena in compressor and turbine components of gas turbine engines

1 Introduction

Quantifying the aerodynamic performance of a turbomachinery component is a highly non-trivial task. It requires the knowledge of multidimensional distributions of various derived flow quantities and thus relies on highly resolved and accurate flow fields, no matter whether they are obtained from experiments or computational fluid dynamics (CFD). Apart from the problem of predicting the flow, a further difficult task is to choose and implement a method to obtain integral quantities such as efficiency or loss parameters. This latter problem, in turn, usually consists in the computation of certain surface averages.

Cumpsty and Horlock [1] gave an excellent overview of the most common ways to compute appropriate average quantities in turbomachinery. They argue that the particular choice of an averaging technique depends on the purpose for which the average is being created and is therefore to a lesser extent a matter of preference. It would, however, be premature to conclude that the choice itself is obvious. For instance, the efficiency of a cooled turbine has been a subject of debate. A multitude of different approaches is analyzed by Young and Horlock [2]. With the introduction of the so-called mechanical work potential, Miller [3] has proposed yet another approach to assess turbine efficiency, thereby questioning the established performance metrics.

Rather than state our own position in this debate, the aim of this paper is to compare the approaches found in Refs. [1–3] and analyze the mechanisms by which they differ. As is shown in this paper, the difference of the approaches can essentially be reduced to the way in which the surface averages involved postulate a certain mixing entropy, i.e., the entropy rise due to averaging. Moreover, one of the keys to understand the different techniques and their impact on performance is the averaging entropy rise which is caused by entropy variations. In particular, we show that this averaging entropy is identical for the work average, the mass-averaged flow mechanical work potential, and, at least approximately, the mixed-out state. Analyses that use increased averaged entropies for the incoming flow yield higher performances. This explains why some of the approaches result in much greater efficiencies than others in the case of cooled turbines.

Moreover, we show that Hartsel's turbine efficiency [4] is closely related to the work average, in that it is compatible with the subdivision and merging of incoming streams. As is shown in this paper, the flow mechanical work potential-based turbine efficiency can be summarized as Hartsel's approach based on work averages with the additional feature of incorporating the so-called reheat effect. This last effect means that losses created locally within the flow at a pressure above the dead-state pressure increase the internal energy and thus the potential to generate shaft work in the subsequent expansion process [3,5].

A further topic is the flux average or mixed-out state which is important for CFD simulations; in that steady Reynolds-averaged Navier–Stokes (RANS) simulations usually rely on conservative formulations of mixing planes, i.e., matching conditions for the radial distributions of circumferentially mixed-out states. In this paper, we use the second-order asymptotic analysis of the flux average mixing entropy [6–8] to relate the flux average in a concise form to the other, more optimistic, averages. In particular, a second-order asymptotic analysis of the work average shows that flux and work average mixing entropies coincide for entropy modes. For vorticity and acoustic modes, however, the second-order approximation of the work average mixing entropy vanishes. Hence, the difference between flux and work averages can be viewed as the potential to decrease mixing losses further downstream, e.g., via the so-called differential work mechanism studied by Rose and Harvey [9] and Rose et al. [10].

Regarding the problem of radial flux averaging, two approaches are discussed here: (i) the so-called *complete radial equilibrium* [11,12] and (ii) a rather simplistic method that generalizes the circumferential averages; this can be computed for any rotational surface but lacks a physical rationale such as an idealized mixing process. As the application shows, both can yield significant mixing entropies which, in contrast to circumferential flux averages, can hardly be justified on the basis of an expected mixing process, especially if subsequent blade rows could, in principle, homogenize reversibly the distorted flow.

The paper is organized as follows. We first revisit the definitions of the different averages in a rather general manner, avoiding

[1]Corresponding author.

Manuscript received July 28, 2022; final manuscript received September 12, 2022; published online November 25, 2022. Tech. Editor: David G. Bogard.

assumptions such as perfect gas. We then analyze the mixing entropies mathematically and illustrate our findings by means of the steady and unsteady flows in a 1.5-stage turbine.

2 Averaging Techniques

In the following, the definitions and the main properties of four important and widely used averaging techniques are outlined. This list, however, is far from being exhaustive. Other commonly used averages are discussed in Ref. [1]. All averages treated in this paper are mass and energy conservative in that the absolute stagnation enthalpy is computed from mass averaging, so that the energy flux equals the average energy flux, i.e., the flux computed from the average values. Note that for a calorically perfect gas, the absolute stagnation enthalpy is proportional to the absolute stagnation temperature.

2.1 Entropy Average. The *entropy* average computes the absolute stagnation pressure from the mass-averaged entropy and absolute stagnation enthalpy [1,11]. It is applicable to flows across all analysis surfaces in a turbomachinery except in certain partial backflow situations which are beyond the scope of this study. The entropy average is optimistic insofar as it is based on the unrealistic assumption that all flow inhomogeneities can mix out without increasing the overall entropy. Note that availability, defined as the specific stagnation exergy $b_t = h_t - T_0 s$ with some reference temperature T_0, is a linear combination of stagnation enthalpy and entropy. Therefore, mass averaging b_t is equivalent to computing b_t from the entropy average, which explains the alternative term *availability average* [1].

2.2 Mechanical Work Potential. To correctly characterize the effect of heat transfer on the work output of a turbine, Miller [3] introduced a measure of the maximum useful work that can be extracted from a fluid by an isentropic turbine exhausting to a given ambient pressure. More precisely, the so-called mechanical work potential is defined as

$$\mathbf{m} = e - e_{se} + p_D(v - v_{se}) + \frac{1}{2}\|U\|^2 = e_t - h_{se} + p_D v$$

whereas the flow mechanical work potential is

$$\mathbf{m}_f = h - h_{se} + \frac{1}{2}\|U\|^2 = h_t - h_{se}$$

Here, the subscript "se" refers to the corresponding value obtained by isentropic expansion to the so-called *dead-state* pressure, denoted by p_D. For example, T_{se} satisfies

$$\int_T^{T_{se}} c_p(T')d\log T' = R\log\left(\frac{p_D}{p}\right)$$

which implies

$$\int_{T_t}^{T_{se}} c_p(T')d\log T' = R\log\left(\frac{p_D}{p_t}\right)$$

since

$$\int_T^{T_t} c_p(T')d\log T' = R\log\left(\frac{p_t}{p}\right)$$

Hence, h_{se} can alternatively be characterized as the *stagnation* enthalpy that is obtained by adiabatically expanding the flow until the *stagnation* pressure attains p_D. Figure 1 illustrates the terms of the flow mechanical work potential drop in real and isentropic expansion processes. The mechanical work potential density can be rewritten in the form

$$\rho\mathbf{m} = \rho e_t - \rho h_{se} - p_D$$

Now, the reference state (denoted by se) is completely determined by the constant value of p_D, the entropy, and the gas composition, i.e.,

$$h_{se} = h(p_D, s, Y_1, \ldots, Y_k)$$

Since s and Y_k satisfy transport equations with diffusion and source terms [13], we obtain a transport equation for h_{se}. The corresponding diffusion and source terms may be derived from

$$\frac{Dh_{se}}{Dt} = \frac{\partial h}{\partial s}\frac{Ds}{Dt} + \sum_k \frac{\partial h}{\partial Y_k}\frac{DY_k}{Dt} = T_{se}\frac{Ds}{Dt} + \sum_k g_{k,se}\frac{DY_k}{Dt} \quad (1)$$

Here, the first partial derivatives are to be understood as derivatives of the enthalpy as a function of s, p and the mass fractions Y_k at $p = p_D$. Note that unlike entropy production, the source term of h_{se} can have both signs. For instance, for a constant composition fluid, we obtain

$$\frac{\partial(\rho h_{se})}{\partial t} + \mathrm{div}[\rho U h_{se}] + T_{se}\mathrm{div}\frac{\vec{q}}{T} = T_{se}\left(\Phi_{visc} - \frac{\vec{q}\cdot\mathrm{grad}T}{T^2}\right) \quad (2)$$

and therefore

$$\frac{\partial(\rho h_{se})}{\partial t} + \mathrm{div}\left[\rho U h_{se} + \frac{T_{se}\vec{q}}{T}\right] = T_{se}\Phi_{visc} + \vec{q}\cdot\mathrm{grad}\frac{T_{se}}{T} \quad (3)$$

Since $\rho e_t - \rho h_{se}$ and $\rho\mathbf{m}$ differ by a constant, the inviscid flux for the conservation law for $\rho\mathbf{m}$ is given by

$$\rho U h_t - \rho U h_{se} = \rho U \mathbf{m}_f$$

Therefore, an (inviscid) flux balance of the mechanical work potential amounts to mass averaging the flow mechanical work potential $\mathbf{m}_f$ which, in turn, amounts to mass averaging h_t and h_{se}.

Mass averaging h_t, Y and $\mathbf{m}_f$ yields *work-potential-based* average values for entropy and stagnation pressure by solving

$$h(p_D, \bar{s}^{mwp}, \overline{Y}^{\dot{m}}) = \overline{h_t}^{\dot{m}} - \overline{\mathbf{m}_f}^{\dot{m}} \quad (4)$$

and computing

$$\bar{p}_t^{mwp} = p(\bar{s}^{mwp}, \overline{h_t}^{\dot{m}}, \overline{Y}^{\dot{m}}) \quad (5)$$

In other words, the work-potential-based average defines a uniform state that would yield the same energy flux, flow mechanical work

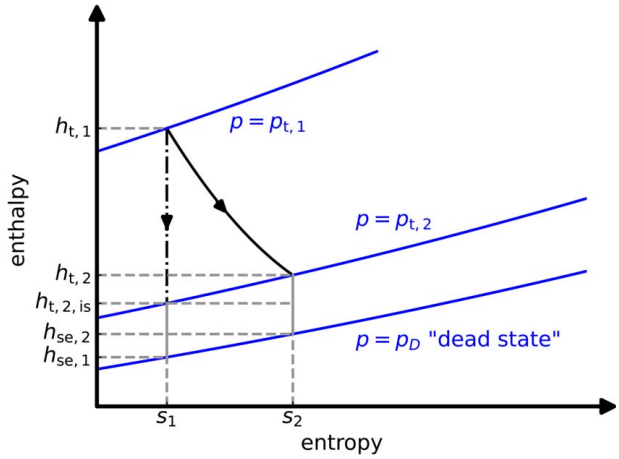

Fig. 1 Enthalpy–entropy chart for real and ideal expansion processes

potential, and overall mass flow, as well as identical species mass flows in the case of multicomponent flow.

Concerning the role of the dead-state pressure, observe that, for thermally perfect gas, two states (p_1, h_1), (p_2, h_2) with identical composition lie on the same isentrope if and only if

$$\int_{h_1}^{h_2} \frac{dh}{RT} = \log \frac{p_2}{p_1} \tag{6}$$

In the case of perfect gas, this implies that replacing p_D with another value $\tilde{p}_D$ means multiplying all values of h_{se} with the constant factor $(\tilde{p}_D/p_D)^{(\gamma-1)/\gamma}$. Therefore, $\bar{s}^{mwp}$ as defined by Eq. (4) is independent of p_D. In the general case of a calorically imperfect gas or a non-constant gas composition, a modified dead-state pressure will result in a value h_{se} which will depend nonlinearly on the original one. Mass averages of this modified h_{se} are therefore expected to give, in general, different values for entropy and stagnation pressure.

2.3 Work Average. The third average discussed here is the work average, which is based on a so-called *work averaged* stagnation pressure [1,11]. Given a distribution of the stagnation quantities p_t, T_t and mass flow densities $d\dot{m}$, the virtual work average mixing process consists in expanding and compressing each infinitesimal streamline to reach a single stagnation pressure, $\overline{p_t}^w$, such that the specific work exerted to or extracted from each streamline integrates to zero. All other thermodynamic quantities are computed from this stagnation pressure and mass-averaged stagnation enthalpy. Since in an adiabatic compression or expansion to $\overline{p_t}^w$, the specific work added is

$$h(\overline{p_t}^w, s, Y) - h_t$$

It follows that the overall flow mechanical work potential vanishes if the dead-state pressure is set to $\overline{p_t}^w$. The flow mechanical work potential is thus a strictly monotonic, continuous function of the dead-state pressure p_D and changes sign when p_D ranges from the minimal to the maximal stagnation pressure. It follows that the work-averaged stagnation pressure is a unique value in this range.

In the case $p_D = \overline{p_t}^w$, the overall flow mechanical work potential is zero, i.e.,

$$\overline{\mathbf{m}_f}^{\dot{m}} = \overline{h_t}^{\dot{m}} - h(\overline{p_t}^w, \bar{s}^{mwp}, \overline{Y}^{\dot{m}}) = 0$$

Hence, $\bar{s}^{mwp}$ is exactly the entropy of the state given by the work-averaged stagnation pressure and the mass averages of the stagnation enthalpy and mass fractions. This means that the mechanical work potential average (cf. Eq. (5)) and the work average give the same stagnation pressure for this particular choice of dead-state pressure. For perfect gas, the mechanical work potential averaged entropy is independent of the dead-state pressure, so, in this case, this equality holds for all dead-state pressures. This fact has already been noted by Miller without further explanation in Ref. [3]. From the arguments in the previous subsection, however, it follows that this identity cannot be expected to hold for a general thermally perfect gas.

To compare work and entropy averages with each other, assume all streamlines have been expanded and compressed isentropically to $\overline{p_t}^w$, as in the virtual experiment explained above. This new distribution agrees with the original one in both averages, so to compare the two averagings, it suffices to consider the case of uniform stagnation pressure. Now,

$$ds = \frac{1}{T_t} dh_t - \frac{1}{\rho_t T_t} dp_t$$

implies that for a given value of p_t, the function $h_t \mapsto s(h_t, p_t)$ has the second derivative $-1/(c_p(T_t)T_t^2)$ and is thus strictly concave. Therefore,

$$\overline{s(h_t, p_t)}^{\dot{m}} \le s(\overline{h_t}^{\dot{m}}, \overline{p_t}^w)$$

with equality if and only if the stagnation enthalpy and thus the entropy are constant (cf. Appendix A). Note that the left-hand side of the inequality corresponds to the entropy computed from the entropy average whereas the right-hand side is the entropy derived from the work average. It follows that the averages are identical for uniform entropy distributions, otherwise the entropy average is more optimistic.

The last argument also shows that for uniform total pressure but varying entropy, entropy averaging yields an increased stagnation pressure. In particular, entropy averaging, in contrast to work averaging, may result in a stagnation pressure outside the range of the input distribution.

2.4 Flux Average. Flux averaging [11] consists of integrating the fluxes and finding a uniform flow state with an identical overall flux. This last step amounts to finding the inverse of the flux function, which may not always have a unique solution. First, both normally subsonic and supersonic solutions may exist. Second, there may be no solution at all, in particular, if the distribution contains partially reversed flow, i.e., the normal flow component changes sign. For small deviations from a uniform state, however, the flux inversion problem is well-posed if the normal flux Jacobian for that uniform state is invertible, i.e., if the normal Mach number is neither zero nor one. In this paper, flux averages are considered only for this non-singular case.

When applying flux averaging to three-dimensional turbomachinery flows, the question of the correct flux components and similarly the velocity components of the uniform state arises. In some situations, it seems natural to choose Cartesian components, and thus search for a state with constant x-, y-, z-components that yield equal Cartesian momentum flux integrals. In turbomachinery, however, this may not be an appropriate method. For instance, consider a rotationally symmetric duct flow. If x is the machine axis, then integrating the y- and z-components of the momentum flux always gives zero. Hence, no information about the swirl and the radial flow component can be extracted from these flux integrals. In this paper, two ways to compute integral flux-averaged values for turbomachinery are discussed.

The first one, which is rather simple to implement, consists in treating the cylindrical components of the flow states as Cartesian, e.g., by setting U^x, U^y, U^z to the axial, radial, and circumferential velocities, respectively. Note that the z-component of the momentum flux coincides, up to a factor of r^{-1}, with the angular momentum flux. Hence, taking a flux average along a line of constant radius, as opposed to rotational surfaces, conserves the angular momentum in that the average state yields the same angular momentum flux as the original distribution. Taking the circumferential flux average for all radii gives a radial distribution of *circumferential* flux averages. In case of an unsteady time periodic flow, one should integrate the fluxes both in time and in the circumferential direction. The relevance of these flux averages for CFD simulations is that the distributions on both sides of a rotor–stator interface have to match if the interface is to be conservative. Mixing planes for steady flow simulations are usually formulated in a conservative fashion [14]. Hence, the mixing entropy due to flux averaging, usually observed as a jump in the circumferentially mass-averaged entropy [7], should be attributed to the steady turbomachinery flow modeling rather than the way the flow is analyzed.

To define a physically more meaningful flux average over a rotational surface, one can seek a *complete radial equilibrium*, i.e., a "mixed-out" radial distribution that corresponds to a steady flow in an annular domain with constant radii and which could at least theoretically be achieved by some virtual dissipation process. An important assumption in these virtual experiments is that the fluxes across the annular walls integrate to zero. In particular, the

walls are assumed inviscid and adiabatic. Pianko and Wazelt [11] and later Prasad [12] describe how the radial equilibrium state can be determined from the integral of axial and angular momenta, the mass flow, and the energy flux through a rotational surface. In contrast to the Cartesian flux average, the flux inversion problem results in a nonlinear equation system that must be solved with an iterative (e.g., Newton) method. Moreover, the approach seems limited to axial turbomachinery. In a narrow annular duct, i.e., with a ratio of outer to inner radii close to 1, this method will coincide with the simple flux average on constant radii described above, since both conserve mass and energy as well as axial and angular momentum.

3 Averaging and Mixing Loss

In the following, the averages defined in the preceding section are analyzed with regard to their inherent mixing entropy, i.e., the entropy rise of work and flux averages when compared to the entropy average:

$$\Delta s^{\mathrm{w}} = \overline{s}^{\mathrm{w}} - \overline{s}^{\dot{m}}, \quad \Delta s^{F} = \overline{s}^{F} - \overline{s}^{\dot{m}}$$

Since the stagnation enthalpy is identical for all averages discussed here and since we assume that the entropy is always consistent with the stagnation quantities, one can easily translate mixing entropies into mixing stagnation pressure losses.

Constant Area Mixing of Two Streams. To illustrate the impact of flux averaging on loss accounting, we consider the entropy rise coefficient

$$\frac{\overline{T}_{\mathrm{t}}\Delta s^{F}}{\overline{h}_{\mathrm{t}} - h_{\mathrm{out}}}, \quad \Delta s^{F} = s_{\mathrm{out}} - \overline{s}^{\dot{m}}_{\mathrm{in}}$$

for the constant area mixing problem of two streams which differ by a given Δp_{t} and ΔT_{t}, as explained, for instance, in the textbook by Greitzer et al. [15, Sec. 5.5] and illustrated in Fig. 2. Here, the value s_{out} is the entropy that results from a virtual mixing process and thus corresponds to the flux-averaged entropy. Figure 3 shows the contours of the entropy rise coefficients for a mean flow Mach number of 0.5. The stagnation pressure difference is non-dimensionalized with the mean compressible dynamic pressure p_{dyn}. The values of the flux average (solid black lines) correspond to the unavoidable entropy rise of a virtual mixing process with adiabatic and inviscid walls. A similar plot containing only the flux-averaged values can be found in Refs. [15,16]. The additional contour lines plotted here correspond to the work-averaged entropy rise Δs^{w} (red dashed lines), i.e., the entropy rise due to work averaging the two inflow streams. In contrast to the mixed-out entropy rise, the

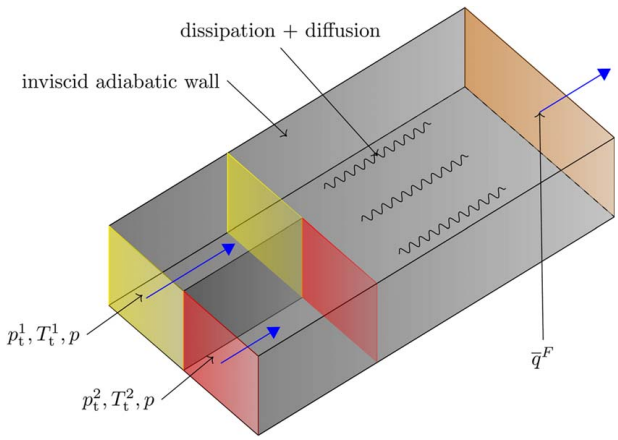

Fig. 2 Virtual mixing process of two streams

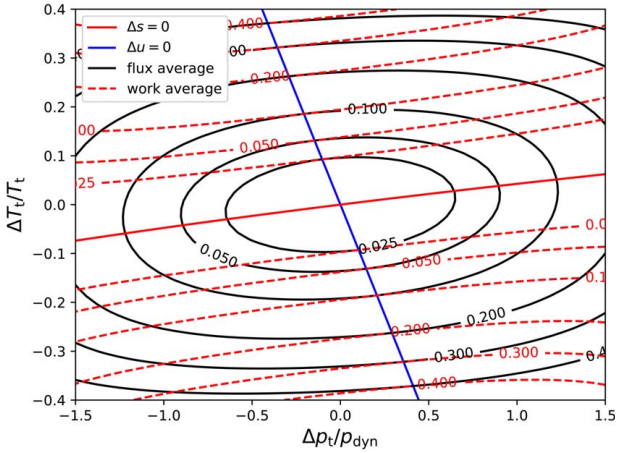

Fig. 3 Constant area mixing loss for two streams with identical pressure and cross-sectional area

entropy rise of work averaging is no longer a strictly convex function. In particular, it is zero along the line of constant entropy variations (red solid line). The blue line corresponds to zero velocity difference. Along this line, the two entropy rise coefficients coincide.

3.1 Second-Order Analysis of Mixing Loss. Recall that the work average can be computed from the mass-averaged dead-state enthalpy h_{se} and the mass-averaged stagnation enthalpy. To approximate the difference between work and entropy average, one can first (cf. Appendix A) estimate

$$\begin{aligned}\overline{h_{\mathrm{se}}}^{\dot{m}} - h(p_{\mathrm{D}}, \overline{s}^{\dot{m}}) &= \overline{h_{\mathrm{se}} - h_{\mathrm{se}}(p_{\mathrm{D}}, \overline{s}^{\dot{m}})}^{\dot{m}} \\ &= \frac{1}{2}\frac{\partial^2 h}{\partial s^2}\Big|_{(\overline{s}^{\dot{m}}, p_{\mathrm{D}})} \overline{(s - \overline{s}^{\dot{m}})^2}^{\dot{m}} + \mathrm{O}((s - \overline{s}^{\dot{m}})^3) \\ &= \frac{T(\overline{s}^{\dot{m}}, p_{\mathrm{D}})}{2c_{\mathrm{p}}} \overline{(s - \overline{s}^{\dot{m}})^2}^{\dot{m}} + \mathrm{O}((s - \overline{s}^{\dot{m}})^3) \end{aligned} \tag{7}$$

This implies the following second-order approximation:

$$\begin{aligned}\Delta s^{\mathrm{w}} &= \frac{\partial s}{\partial h}\Big|_{(h(\overline{s}^{\dot{m}}, p_{\mathrm{D}}), p_{\mathrm{D}})} (\overline{h_{\mathrm{se}}}^{\dot{m}} - h_{\mathrm{se}}(\overline{s}^{\dot{m}})) + \mathrm{O}((\overline{h_{\mathrm{se}}}^{\dot{m}} - h_{\mathrm{se}}(\overline{s}^{\dot{m}}))^2) \\ &= \frac{1}{2c_{\mathrm{p}}} \overline{(s - \overline{s}^{\dot{m}})^2}^{\dot{m}} + \mathrm{O}((s - \overline{s}^{\dot{m}})^3) \end{aligned}$$

which can be rewritten in terms of non-dimensionalized entropies in the form

$$\frac{\Delta s^{\mathrm{w}}}{R} \approx \frac{1}{2}\frac{\gamma - 1}{\gamma} \overline{(s/R - \overline{s}^{\dot{m}}/R)^2}^{\dot{m}} \tag{8}$$

For circumferential flux averages, we have the second-order expansion

$$\Delta s^{F} = \sum_{\omega,m,l} \Delta s^{F}_{\omega,m,l} + \mathrm{O}(\|q - \overline{q}\|^3) \tag{9}$$

where $\Delta s^{F}_{\omega,m,l}$ is the approximate entropy rise attributed to the lth mode of the harmonic with angular frequency ω and the circumferential mode order m [7]. $\Delta s^{F}_{\omega,m,l}$ is the unavoidable mixing loss that would occur if this mode dissipated in some process that conserves mass, momentum, and energy. l runs over the five mode types (entropy, two vorticity, and two acoustic modes). Schlüß and

Frey [8] show that

$$\Delta s^F_{\omega,m,l} = \frac{1}{2\dot{m}\Delta t} v_g \cdot \int_{t_0}^{t_0+\Delta t} \int_\Gamma \langle q', q' \rangle_{\rho s} dA \, dt \tag{10}$$

for all but cutoff acoustic modes (see Eq. (B2) of Appendix B). Here, v_g is the normal group velocity of the corresponding mode type, q' is the disturbance of the Fourier harmonic, projected onto the line spanned by the lth right-eigenvector of the dispersion relation. The inner product $\langle q', q' \rangle_{\rho s}$ is the inner product associated to the Hessian of the entropy density (see Eq. (B1)). For an infinitesimal entropy mode, we have

$$\frac{\rho'}{\rho} = -\frac{s'}{c_p}$$

and p' as well as U' vanish. Hence, using Eq. (B1),

$$\frac{\Delta s^F_{\omega,m,1}}{R} = \frac{1}{2}\frac{\overline{|s'|^2}}{c_p R} = \frac{1}{2}\frac{\gamma - 1}{\gamma}\overline{(s'/R)^2}$$

which is, up to third order, identical with the second-order approximation of the work average mixing entropy, i.e., the right-hand side of Eq. (8).

Observe that for cutoff acoustic modes, the left-hand side of Eq. (10) is zero, if only left- or only right-running modes have non-zero amplitudes. In case both are present, there is an additional term that intertwines cutoff modes, see Ref. [8] for details.

4 Turbine Efficiency

One of the standard definitions of turbine efficiency for configurations with coolant streams goes back to Hartsel [4]:

$$\eta^{\text{Hart}} = \frac{\dot{m}\left(\overline{h}^{\dot{m}}_{t_{in}} - \overline{h}^{\dot{m}}_{t_{out}}\right)}{\sum_i \dot{m}_i \left(\overline{h}^{\dot{m}}_{t_{in},i} - h_{t,out,is,i}\right)} \tag{11}$$

where $h_{t,out,is,i}$ is computed from the ith mass-averaged stagnation enthalpy and appropriately averaged inflow and outlet stagnation pressures. More precisely, $h_{t,out,is,i}$ is the stagnation enthalpy that is obtained if the ith stream is adiabatically expanded until the stagnation pressure attains $\overline{p}_{t,out}$. i runs over all inflows including the main gas flow and the coolant streams. For an uncooled turbine, this definition reduces to the standard isentropic "total-to-total" efficiency η^{tt} [2].

For cooled turbines, Young and Horlock [2] suggest to use a so-called *fully reversible* efficiency where an ideal mixing process is thought to mix out the main gas flow and the coolant streams without generating entropy. Using the nomenclature of this paper, this so-called *fully reversible* efficiency, denoted by η^{fr}, is just the standard single-stream efficiency in Eq. (11) with inflow values defined as an entropy average over the main inflow and all coolant streams. Since it is shown above that the difference between work and entropy averages is essentially a function of the entropy variation, with a second-order approximation of the difference given by Eq. (8), we see that the fully reversible analysis does not differ much from the work-averaged total-to-total analysis unless there are significant entropy variations. However, if secondary inflows with much lower entropy exist, then this difference is responsible for the highly optimistic fully-reversible average inflow state which, as a consequence, leads to a relatively low efficiency. This phenomenon is illustrated with an academic example below. A similar behavior is expected for unsteady flows in high-pressure turbines with the migration of hot streaks.

The mechanical work potential-based efficiency is defined as the ratio between the specific work extraction and the mechanical work potential drop [3]:

$$\eta^{\text{mwp}} = \frac{\overline{h}^{\dot{m}}_{t_{in}} - \overline{h}^{\dot{m}}_{t_{out}}}{\overline{\mathbf{m}}^{\dot{m}}_{f_{in}} - \overline{\mathbf{m}}^{\dot{m}}_{f_{out}}} \tag{12}$$

Note that all the different turbine efficiencies may be written in the form

$$\eta = \frac{P_{\text{gross}}}{P_{\text{ideal}}} = \frac{P_{\text{gross}}}{P_{\text{gross}} + P_{\text{loss}}} \tag{13}$$

with $P_{\text{gross}} = \dot{m}(\overline{h}^{\dot{m}}_{t,in} - \overline{h}^{\dot{m}}_{t,out})$ being the gross power output. P_{ideal} is the corresponding denominator. $P_{\text{loss}} = P_{\text{ideal}} - P_{\text{gross}}$ is the difference between the ideal and the actual power output and represents the "lost" power. Now, Hartsel's definition can be expressed as

$$P^{\text{Hart}}_{\text{loss}} = \sum_i \dot{m}_i \left(h(\overline{s}_{\text{out}}, \overline{p}_{t,\text{out}}) - h(\overline{s}_{\text{in},i}, \overline{p}_{t,\text{out}})\right)$$

where the average bars indicate one particular averaging type. In the limit of infinitely many streamlines, this formula converges to the lost power modeled in the mechanical work potential-based analysis

$$P^{\text{mwp}}_{\text{loss}} = \int (h_{se,\text{out}} - h_{se,\text{in}}) d\dot{m}$$

with dead-state pressure $p_D = \overline{p}_{t,\text{out}}$. The above integral is to be taken over all streamlines. Hence,

$$P^{\text{mwp}}_{\text{loss}} = \iint_{s_{\text{in}}}^{s_{\text{out}}} T_{se} \mathrm{d}s \, d\dot{m} \tag{14}$$

Since in the case of a perfect gas, the mechanical work potential-based average coincides with the work average, we can interpret Hartsel's efficiency using work averages as the mechanical work potential-based efficiency with a particular choice for the dead-state pressure. Moreover, Hartsel's efficiency is compatible with work averages in the sense that it is invariant under the subdivision or merging of inflows as long as the work average is used.

The important feature of the mechanical work potential-based efficiency analysis with a general dead-state pressure is to take into account the so-called reheat effect. Since

$$P^{\text{mwp}}_{\text{loss}} = \iint_{s_{\text{in}}}^{s_{\text{out}}} \frac{T^{p_D}_{se}}{T^{\overline{p}^{w}_{t,\text{out}}}_{se}} T^{\overline{p}^{w}_{t,\text{out}}}_{se} \mathrm{d}s \, \mathrm{d}\dot{m} \tag{15}$$

each local entropy production appearing in the work-averaged total-to-total analysis is thus reduced by a factor of

$$\frac{T^{p_D}_{se}}{T^{\overline{p}^{w}_{t,\text{out}}}_{se}} = \frac{T^{p_D}_{se}}{\overline{T}^{w}_{t,\text{out}}}$$

Here, the superscript marks which dead-state pressure is to be used. Miller argues that the lost power modeled in the other efficiency analyses is not necessarily completely lost but corresponds to heat that can be converted into useful work by subsequent turbine stages, the optimal work extraction being given by the Joule-cycle efficiency [3,5].

Summarizing, two very different effects are responsible for the mechanical work potential-based analysis to yield, for high-pressure turbines, much greater efficiencies than the fully reversible analysis by Young and Horlock [2]. First, the mechanical work potential-based averaging attributes a high mixing entropy to inflows with strong entropy variation. Second, the mechanical work potential-based efficiency takes into account the reheat effect.

Both Hartsel's and Miller's approach can be viewed as a loss analysis which is based on the dead-state enthalpy h_{se} with an appropriately chosen dead-state pressure. Since h_{se} corresponds to the inviscid flux of a nonlinear function of the entropy (and composition in case of variable gas mixtures), one cannot expect h_{se} to always increase. Indeed, both Miller [3] and Young and Horlock

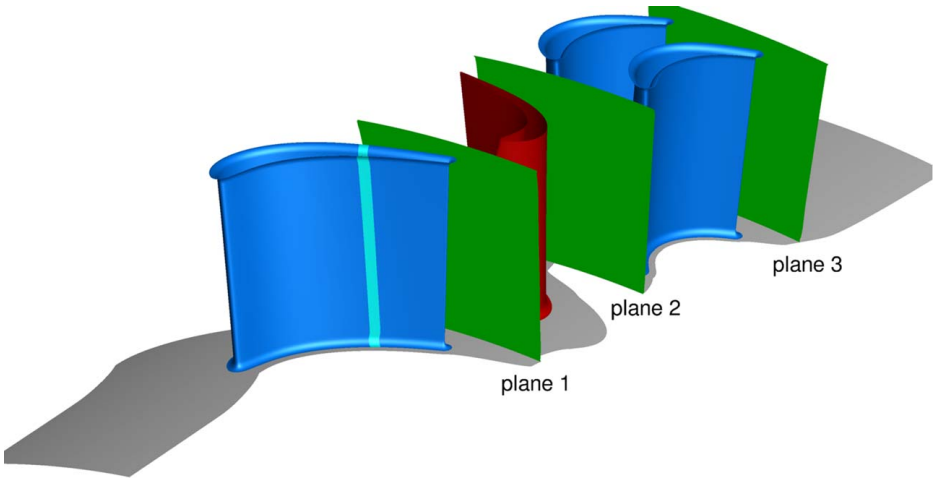

Fig. 4 Aachen cold air turbine test case with measurement planes (green)

[2] give academic examples of configurations with negative losses for the corresponding approaches.

5 Implementation

All techniques described here have been implemented in the post-processing tool of DLR's in-house CFD software TRACE. The post-processor carries out a chain, or more generally a directed graph, of elementary tasks (input/output, computation of integrals or derived quantities, etc.). The averaging process essentially consists of tasks that compute (i) flux integrals, mass flow weighted integrals, etc. over surfaces and bands of nearly constant radius and (ii) tasks that compute flow states and derived quantities from these integrals. For unsteady flow simulations, the integrals are computed and summed up inside a loop over time instances which preferably are the solver time-steps of a time period. For frequency domain simulations, the time instances should be chosen to be the sampling points of the harmonic balance (HB) formulation (see Refs. [17,18] for the method used here). This way, consistency with the numerical boundary conditions is achieved.

6 Test Case

To illustrate the properties of different averagings and their impact on efficiency, the flow through the 1.5 stage cold air turbine rig operated by the Institute of Jet Propulsion and Turbomachinery at RWTH Aachen is simulated and analyzed. Experimental data from five-hole probes for this case have been compared to steady and unsteady TRACE results in the past by Restemeier et al. [19] who found that unsteady RANS simulations showed better agreement between numerical and experimental results. An overview of the configuration employed here is given in Fig. 4. The configuration is identical to that used by Morsbach [20]. The results of two steady and one harmonic balance simulation are analyzed. The second steady simulation is purely academic and differs from the first by the injection of cold air along strips on the first stator's pressure and suction sides, marked in light blue in Fig. 4. The overall cooling mass flow is 4% of the main inflow. The coolant total temperature is about 50% lower than that at the main inflow. Since the fluid is modeled as perfect gas, one should think of this flow as being representative of much higher temperatures since, for instance, phase transitions expected for CO_2 at the temperatures here are simply discarded. The motivation for this setup, called "cooled" in the following, is to illustrate the impact of high entropy variations in the inflows as they typically occur in cooled high-pressure turbines. The third, uncooled configuration is a harmonic balance simulation [18] with three harmonics for each rotor–stator interaction. The second stator row consists of two passages to account for the clocking effect between stators 1 and 2. All simulations are fully turbulent and use Menter's shear stress transport (SST) turbulence model in a log ω-formulation.

Figures 5 and 6 show the distributions of streamwise vorticity and Mach number as measured by the five-hole probes in comparison with the steady uncooled CFD result. As observed in the literature, the configuration shows relatively pronounced secondary flow structures [21]. The area-averaged axial velocity of the steady and unsteady simulations is compared with the experimental data in Fig. 7. The overall agreement between numerical and

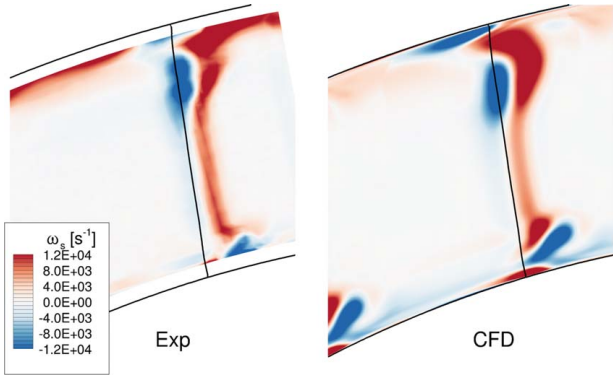

Fig. 5 Streamwise vorticity at measurement plane between first stator and rotor. Steady CFD versus experiment.

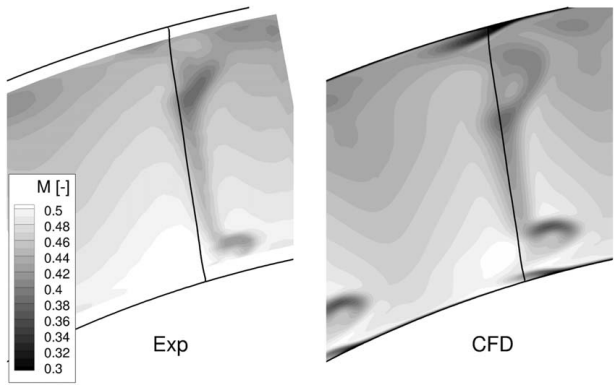

Fig. 6 Mach number at plane 1. Steady CFD versus experiment.

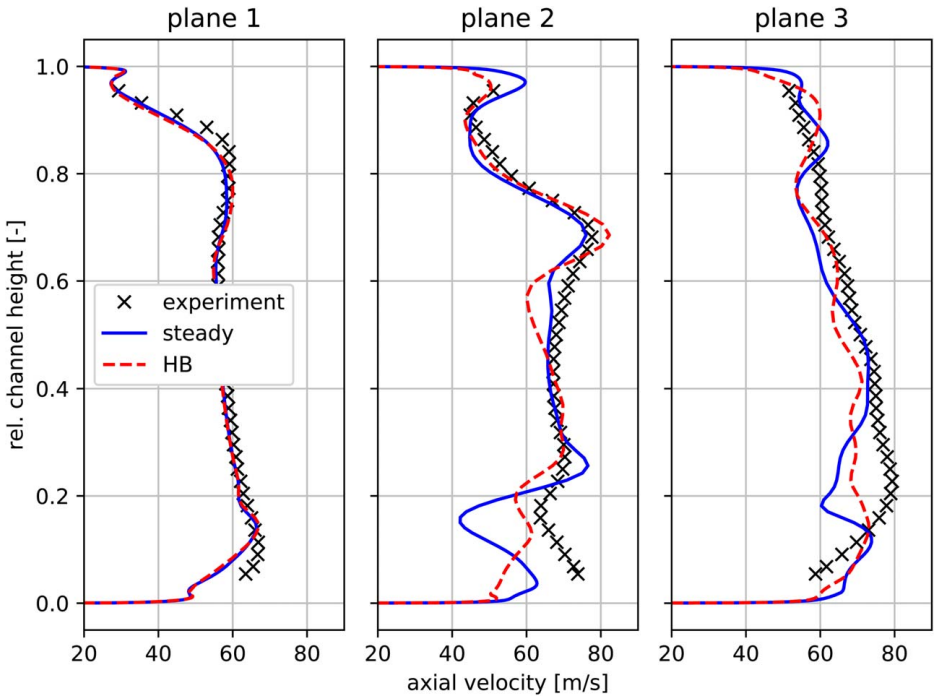

Fig. 7 Circumferentially averaged axial velocity at measurement planes. CFD versus experiments.

experimental data highlights that the flow solutions used here are not only representative of CFD results but also of real turbomachinery flow fields.

The mixing entropy of flux and work averages has been analyzed for the steady simulations at the outlet of the first stator and, for the uncooled simulation, for the outlet of the rotor, see Fig. 8. The second-order approximations (i) for all modes and (ii) for the entropy mode alone (cf. Eqs. (8) and (9)) are plotted in gray and show a good agreement with the flux and work average mixing entropies, respectively. Somewhat higher discrepancies can be seen for the cooled configuration. Figure 9 shows the entropy distributions for cooled and uncooled setups along the first stator outlet. A strong entropy variation that causes an additional mixing entropy in the order of magnitude of the vorticity modes can be seen for the cooled setup. In the uncooled case, work and entropy averages show no significant difference. These results are consistent with our findings in the section on constant area mixing (see Fig. 3). Whenever the entropy variation is small, the work average has no significant mixing entropy. In case of high entropy variations, the mixing entropy due to work averaging may attain values that are comparable in magnitude to that of flux averaging.

Finally, to study integral quantities, different radial averaging procedures are shown in Fig. 10 and compared in terms of entropy. The solid lines correspond to the circumferential averages of the uncooled steady CFD at the outlets of the first stator and the rotor, and the dashed lines represent a certain radial average. The blue solid line corresponds to the complete radial equilibrium (denoted by "rad eq") computed with Prasad's procedure [12], the

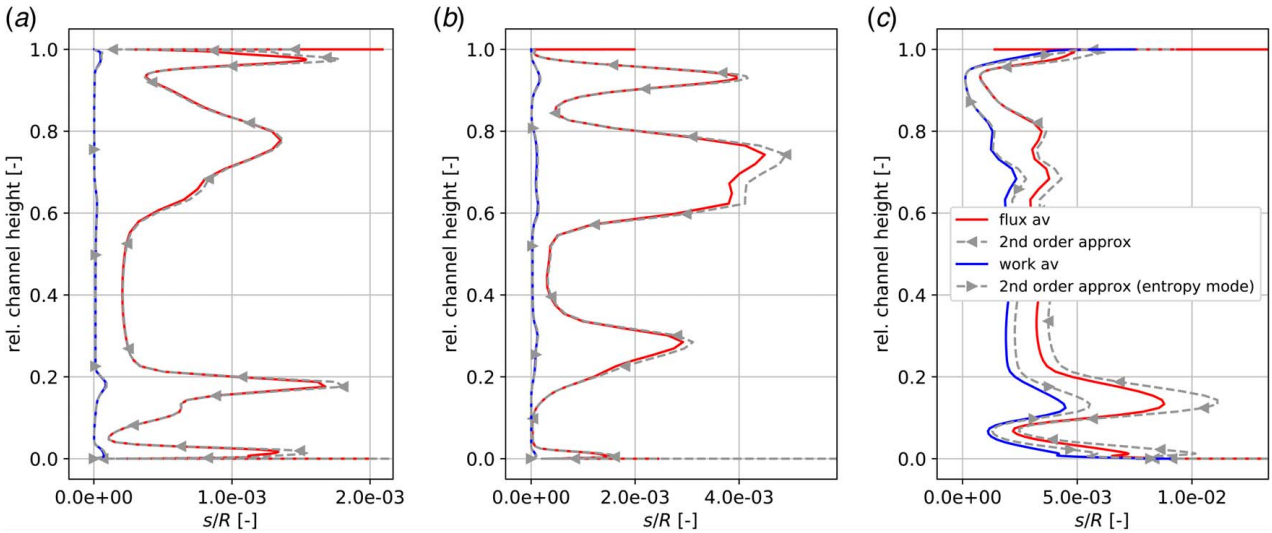

Fig. 8 Mixing entropies for uncooled ((*a*) and (*b*)) and cooled (*c*) steady CFD: (*a*) Stator 1 outlet, (*b*) Rotor outlet, and (*c*) Stator 1 outlet ("cooled").

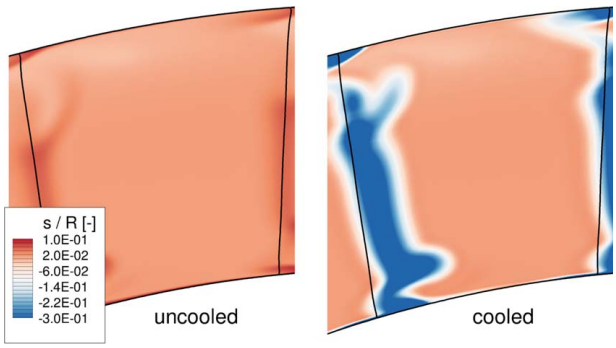

Fig. 9 Entropy at plane 1. Uncooled versus cooled configuration.

dashed blue line being its radial entropy average. The red dashed line represents the integral value computed with the simplistic flux average method outlined above (denoted by "flux/flux av"). When compared with the radially work-averaged circumferential flux average ("flux/work av"), both radial flux averaging procedures can result in a significant additional mixing entropy, as can be seen in particular for the rotor outlet. Note that the additional entropy caused by taking the complete equilibrium can hardly be linked to the unavoidable mixing entropy of an idealized mixing process inside the present configuration as the neighboring blade rows could be designed in such a way that they largely homogenize the radial distribution of the flow. In situations where there is no potentially rectifying structure, e.g., for flows into propelling nozzles, other approaches such as the so-called *thrust average* should be considered [1]. At the stator outlet, the "simplistic" flux averaging

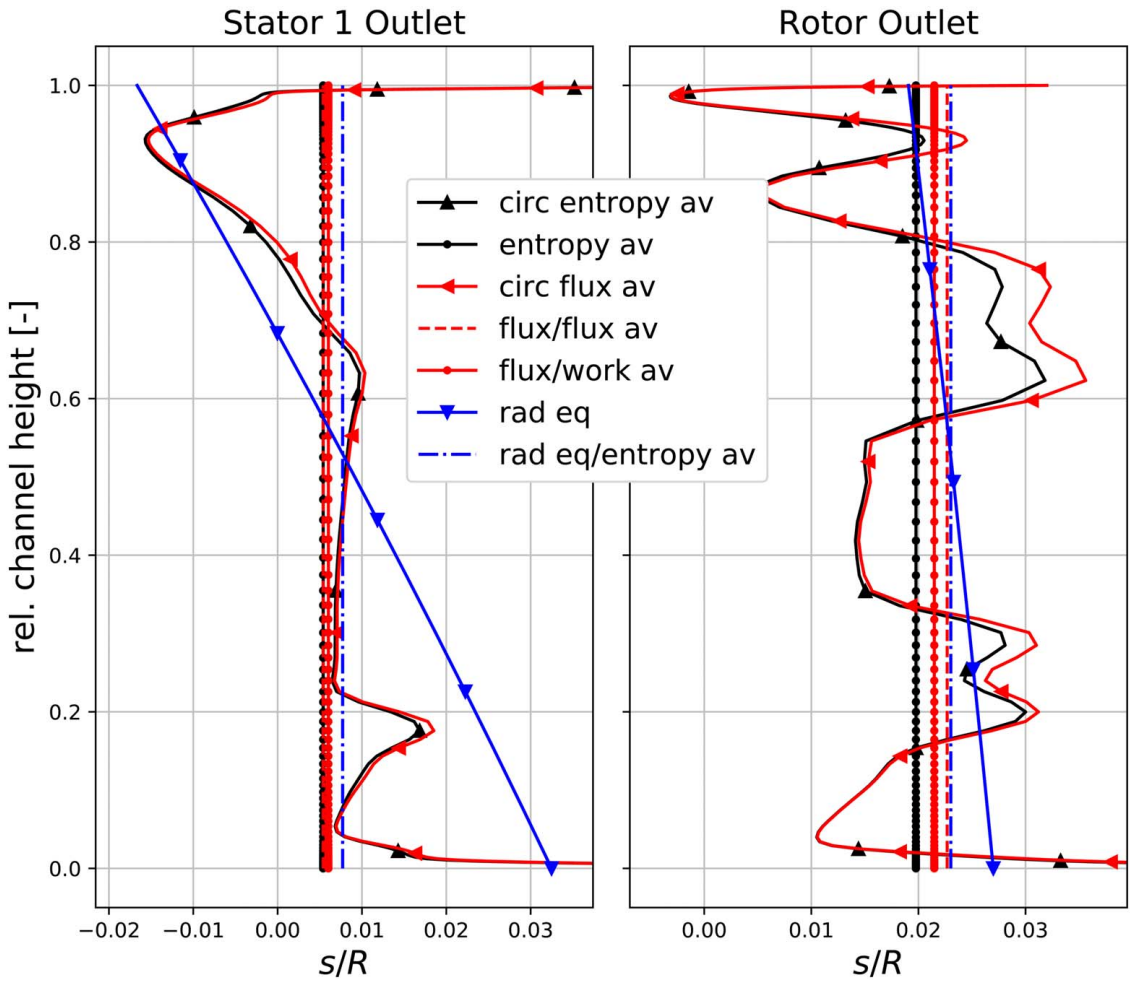

Fig. 10 Entropy (black) flux averages (red), complete radial equilibrium (blue), and their radial averages (dashed). Steady uncooled configuration.

Table 1 Comparison of efficiency definitions for first stage

	η^{Hart}				η^{mwp}		
	Work av	Entropy av	Flux/work av	Flux/flux av	$p_{\mathrm{D}} = \overline{p_{\mathrm{t,R}}}^{\mathrm{w}}$	$p_{\mathrm{D}} = \overline{p}^{\mathrm{w}}_{\mathrm{S2}}$	η^{fr}
Steady	0.00%	0.02%	−0.58%	−0.99%	0.00%	0.20%	0.02%
HB	−0.18%	−0.18%	−1.10%	−1.44%	−0.18%	0.02%	−1.18%
"Cooled"	−1.54%	−1.52%	−2.06%	−2.37%	−1.54%	−1.30%	−9.23%

approach ("flux/flux av") yields a negative mixing entropy which indicates that this radial flux average does not correspond to some uniform flow state that could be attained far downstream after sufficient diffusion and dissipation.

Table 1 lists the efficiencies of the first stage (first stator and rotor) as predicted by three simulations. The values shown correspond to the difference between the result and the steady uncooled work-averaged-based analysis. The efficiency is computed with different approaches (Hartsel, mechanical work potential, and "fully reversible" analysis) and in the case of Hartsel's efficiency using different averaging techniques. The results show for all configurations that if the dead-state pressure is set to the work-averaged outlet stagnation pressure, the mechanical work potential-based efficiency coincides with Hartsel's efficiency using work averages. Moreover, if the dead-state pressure is set to the exit static pressure behind the second stator, a slight increase is seen for the mechanical work potential-based efficiency. The fully reversible analysis gives the same value as the entropy average-based analysis for uncooled configurations. In contrast, the work average type mixing of the different streams in case of Hartsel's approach show significantly higher efficiencies than the fully reversibly analysis for the cooled configuration. Finally, flux averaging results in the well-known efficiency drop. A further decrease in performance is predicted when the flux average is applied in the radial direction as well.

7 Conclusions

In this paper, various common averaging techniques have been studied with regard to their mathematical properties, underlying rationales, and relationships between them. The flow mechanical work potential is found to be closely related to the work average. As has been stated earlier in the literature, the corresponding averages are identical for perfect gas. The additional important feature of work potential-based analysis is that it relates the losses to the capability of a Joule cycle to convert the generated heat into useful work. For non-constant gas properties, the mechanical work potential-based averages depend on the dead-state pressure although the relevance of this dependency for practical applications has not been worked out here and should be the subject of future studies.

The averages have been compared in this article in terms of their mixing loss, i.e., the entropy difference between the mass-averaged entropy and the entropy calculated from the particular averaging. It is shown that the work average is always equally or more pessimistic than the entropy average, with equality only for distributions that are isentropic and have constant gas composition. For constant gas composition, the entropy rise due to flux averaging can be approximated up to second order with respect to the disturbance amplitudes. This quadratic approximation, in turn, can be decomposed into contributions from different disturbance types (entropy, vorticity, and acoustic modes). It is found that a corresponding asymptotic analysis for the work average yields mixing losses that are identical to those of flux averaging for entropy modes, but vanish for vorticity and acoustic modes. Hence, Cumpsty and Horlock's conclusion that in turbomachinery practice, entropy and work averages will not differ much can be expressed in a mathematically precise way as follows. The additional work average loss is approximately proportional to the second moment of entropy in the input distribution.

Taking the complete radial equilibrium of flux averages can result in a significant mixing entropy that in the context of a turbomachinery design seems overly pessimistic. In contrast, radial distributions of temporally and circumferentially flux-averaged quantities are compatible with the flow modeling of steady mixing plane simulations and therefore appropriate for their analysis. Taking the entropy or work average of these radial distributions limits the pessimism of flux averagings to circumferential and temporal disturbances. The mixing entropy due to this hybrid averaging can be taken as a measure of the modeled mixing losses that are due to the mixing plane approach and which could potentially decrease if unsteady effects were taken into account.

Conflict of Interest

There are no conflicts of interest.

Data Availability Statement

The authors attest that all data for this study are included in the paper.

Nomenclature

e = internal energy
g = Gibbs energy
h = enthalpy
$\dot{m}$ = mass flow
p = pressure
$\vec{q}$ = heat flux
s = entropy
t = time
v = specific volume
$\mathbf{i}$ = imaginary unit
$\mathbf{m}$ = mechanical work potential
R = specific gas constant
T = temperature
U = velocity vector
$\mathbf{m}_\mathrm{f}$ = flow mechanical work potential
$\mathbf{D}f$ = Jacobian of f
$\mathbf{H}f$ = Hessian of f
c_v, c_p = specific heat capacities
X_k, Y_k = mole and mass fractions

Greek Symbols

γ = specific heat ratio
ρ = density
Φ_visc = viscous dissipation rate
ω = angular frequency

Subscripts

D = dead state
se = value after adiabatic expansion to dead-state pressure
t = stagnation quantity

Superscripts

F = flux average
fr = fully reversible (efficiency)
is = isentropic
$\dot{m}$ = mass average
mwp = mechanical work potential
tt = total-to-total (efficiency)
w = work average

Appendix A: Second-Order Asymptotics of Averages

Consider n state variables $q_1, \ldots, q_n$ and a derived quantity $y = f(q)$ where f is a smooth, possibly nonlinear function. The comparison of averaging techniques can be boiled down to the problem of finding the difference between (i) averaging y and (ii) computing y from average quantities $\overline{q}$. For simplicity, assume that the averaging is mass-weighted although the following arguments are more general. For an analysis surface Γ, we have the following

consequence of Taylor's theorem:

$$\begin{aligned}\overline{y} - f(\overline{q}) &= \frac{1}{\dot{m}}\int_\Gamma \big(f(q) - f(\overline{q}^{\dot{m}})\big)d\dot{m} \\ &= \frac{1}{\dot{m}}\int_\Gamma \mathbf{D}f(\overline{q}^{\dot{m}})[q - \overline{q}^{\dot{m}}] \\ &\quad + \frac{1}{2}(q - \overline{q}^{\dot{m}})^{\mathrm{T}}\mathbf{H}f(\overline{q}^{\dot{m}})(q - \overline{q}^{\dot{m}})d\dot{m} + \mathrm{O}(\|q - \overline{q}^{\dot{m}}\|_\infty^3) \\ &= \frac{1}{2}\overline{(q - \overline{q}^{\dot{m}})^{\mathrm{T}}\mathbf{H}f(\overline{q}^{\dot{m}})(q - \overline{q}^{\dot{m}})}^{\dot{m}} + \mathrm{O}(\|q - \overline{q}^{\dot{m}}\|_\infty^3)\end{aligned}$$

where $\mathbf{D}f$ and $\mathbf{H}f$ denote the Jacobian and Hessian of f. Hence, up to third order, the second derivative of f at $\overline{q}^{\dot{m}}$ determines the difference of the averaging processes. Moreover, using the integral form for the remainder term of the first-order Taylor expansion, we have

$$\begin{aligned}f(q) - f(\overline{q}^{\dot{m}}) &= \mathbf{D}f(\overline{q}^{\dot{m}})[q - \overline{q}^{\dot{m}}] \\ &\quad + \int_0^1 (q - \overline{q}^{\dot{m}})^{\mathrm{T}}\mathbf{H}f((1-t)\overline{q}^{\dot{m}} + tq)(q - \overline{q}^{\dot{m}})(1-t)dt\end{aligned}$$

Since the average of the linear term vanishes, we have

$$\overline{y} - f(\overline{q}^{\dot{m}}) = \int_0^1 \overline{(q - \overline{q}^{\dot{m}})^{\mathrm{T}}\mathbf{H}f((1-t)\overline{q}^{\dot{m}} + tq)(q - \overline{q}^{\dot{m}})}^{\dot{m}}(1-t)\,\mathrm{d}t$$

This last equation shows that the difference is always positive (negative), if the Hessian $\mathbf{H}f$ is positive (negative) definite. This corresponds to the case of a strictly convex (concave) function f.

Appendix B: Asymptotic Expansion of Mixing Losses

For two-dimensional time periodic ideal gas flow, Fritsch [6] and Fritsch and Giles [7] first presented an asymptotic mixing loss formula in the form of Eq. (9). Schlüß and Frey [8] recovered this formula and showed that it is a consequence of the fact that the Euler equations form a hyperbolic system and possess a convex entropy–entropy flux pair. The general formula in Ref. [8] expresses each summand in terms of the normal group velocity v_g and the square of a certain norm of the disturbance amplitude of the corresponding mode. This squared norm is the inner product defined by the Hessian of the entropy density as a function of conserved quantities. With primitive components ρ_i', U_i', p_i', this inner product is given by

$$\langle q_1', q_2'\rangle_{\rho s} = c_\mathrm{v}\rho \begin{pmatrix} \rho_1'/\overline{p}^{\mathrm{a}} \\ U_1'/\overline{a}^{\mathrm{a}} \\ p_1'/\overline{p}^{\mathrm{a}} \end{pmatrix}^{\mathrm{H}} \begin{pmatrix} \gamma & 0 & -1 \\ 0 & \gamma(\gamma-1) & 0 \\ -1 & 0 & 1 \end{pmatrix} \begin{pmatrix} \rho_2'/\overline{p}^{\mathrm{a}} \\ U_2'/\overline{a}^{\mathrm{a}} \\ p_2'/\overline{p}^{\mathrm{a}} \end{pmatrix} \tag{B1}$$

Here, $\overline{a}^{\mathrm{a}}$ and $\overline{p}^{\mathrm{a}}$ denote the velocity of sound and pressure derived from the area-averaged state $\overline{q}^{\mathrm{a}}$. The second-order approximate contribution to the mixing entropy of the lth mode can now be expressed as

$$\Delta s^F_{\omega,m,l} = \frac{1}{2\dot{m}\Delta t} v_\mathrm{g} \cdot \int_{t_0}^{t_0+\Delta t}\int_\Gamma \langle q' q'\rangle_{\rho s}\,\mathrm{d}A\,\mathrm{d}t \tag{B2}$$

with Δt being the time period. When the up- and downstream cutoff acoustic modes with identical frequencies and mode orders have both non-zero amplitudes, they give an additional contribution which, as shown in Ref. [8], must therefore be taken into account for unsteady simulations of rotor–stator interactions.

References

[1] Cumpsty, N. A., and Horlock, J. H., 2006, "Averaging Nonuniform Flow for a Purpose," ASME J. Turbomach., **128**(1), pp. 120–129.
[2] Young, J. B., and Horlock, J. H., 2006, "Defining the Efficiency of a Cooled Turbine," ASME J. Turbomach., **128**(4), pp. 658–667.
[3] Miller, R. J., 2013, "Mechanical Work Potential," ASME Turbo Expo: Power for Land, Sea, and Air, Vol. 6A, San Antonio, TX, June 3–7, p. V06AT36A032.
[4] Hartsel, J. E., 1972, "Prediction of Effects of Mass-Transfer Cooling on the Blade-Row Efficiency of Turbine Airfoils," AIAA, 10th Aerospace Sciences Meeting, San Diego, CA, Paper No. AIAA-72-11.
[5] Jardine, L., and Miller, R., 2021, "The Effect of Heat Transfer on Turbine Performance," ASME J. Turbomach., pp. 1–34.
[6] Fritsch, G., 1992, "An Analytical and Numerical Study of the Second-Order Effects of Unsteadiness on the Performance of Turbomachines," Ph.D. thesis, Massachusetts Institute of Technology, Cambridge, MA.
[7] Fritsch, G., and Giles, M. B., 1995, "An Asymptotic Analysis of Mixing Loss," ASME J. Turbomach., **117**(3), pp. 367–374.
[8] Schlüß, D., and Frey, C., 2018, "Mixing Losses in Steady and Unsteady Simulations of Turbomachinery Flows," ASME Turbo Expo: Power for Land, Sea, and Air, Vol. 2C, Oslo, Norway, June 11–15, p. V02CT42A014.
[9] Rose, M. G., and Harvey, N. W., 2000, "Turbomachinery Wakes: Differential Work and Mixing Losses," ASME J. Turbomach., **122**(1), pp. 68–77.
[10] Rose, M., Schüpbach, P., and Mansour, M., 2013, "The Thermodynamics of Wake Blade Interaction in Axial Flow Turbines: Combined Experimental and Computational Study," ASME J. Turbomach., **135**(3), p. 031015.
[11] Pianko, M., and Wazelt, F., 1983, "Suitable Averaging Techniques in Non-Uniform Internal Flows," Tech. Rep., AGARD AR, Propulsion and Energetic Panel Working Group, No. 182.
[12] Prasad, A., 2005, "Calculation of the Mixed-Out State in Turbomachine Flows," ASME J. Turbomach., **127**(3), pp. 564–572.
[13] Giovangigli, V., 1999, *Multicomponent Flow Modeling*, Birkhäuser, Boston, MA.
[14] Giles, M., 1991, "UNSFLO: A Numerical Method for the Calculation of Unsteady Flow in Turobmachinery," Tech. Rep., Gas Turbine Laboratory Report GTL 205, MIT Dept. of Aero. and Astro.
[15] Greitzer, E. M., Tan, C. S., and Graf, M. B., 2004, *Internal Flow*, Cambridge University Press, New York.
[16] Denton, J. D., 1993, "The 1993 IGTI Scholar Lecture: Loss Mechanisms in Turbomachines," ASME J. Turbomach., **115**(4), pp. 621–656.
[17] Frey, C., Ashcroft, G., Kersken, H.-P., and Voigt, C., 2014, "A Harmonic Balance Technique for Multistage Turbomachinery Applications," ASME Turbo Expo 2014: Turbine Technical Conference and Exposition, Düsseldorf, Germany, June 16–20, p. V02BT39A005.
[18] Frey, C., Ashcroft, G., Kersken, H.-P., Schönweitz, D., and Mennicken, M., 2018, "Simulation of Indexing and Clocking With Harmonic Balance," Int. J. Turbomach. Propul. Power, **3**(1), p. 1.
[19] Restemeier, M., Jeschke, P., Guendogdu, Y., and Gier, J., 2012, "Numerical and Experimental Analysis of the Effect of Variable Blade Row Spacing in a Subsonic Axial Turbine," ASME J. Turbomach., **135**(2), p. 021031.
[20] Morsbach, C., 2016, *Reynolds Stress Modelling for Turbomachinery Flow Applications*, Dissertation, TU Darmstadt, Darmstadt, Germany.
[21] Poehler, T., Niewoehner, J., Jeschke, P., and Guendogdu, Y., 2015, "Investigation of Nonaxisymmetric Endwall Contouring and Three-Dimensional Airfoil Design in a 1.5-Stage Axial Turbine—Part I: Design and Novel Numerical Analysis Method," ASME J. Turbomach., **137**(8), p. 081009.